

## Electronic structure of ellipsoidally deformed quantum dots

This article has been downloaded from IOPscience. Please scroll down to see the full text article.

2001 J. Phys.: Condens. Matter 13 1987

(<http://iopscience.iop.org/0953-8984/13/9/321>)

View [the table of contents for this issue](#), or go to the [journal homepage](#) for more

Download details:

IP Address: 171.66.16.226

The article was downloaded on 16/05/2010 at 08:46

Please note that [terms and conditions apply](#).

## Electronic structure of ellipsoidally deformed quantum dots

In-Ho Lee<sup>1</sup>, Yong-Hoon Kim<sup>2</sup> and Kang-Hun Ahn<sup>3</sup>

<sup>1</sup> School of Physics, Korea Institute for Advanced Study, Cheongryangri-dong, Dongdaemun-gu, Seoul 130-012, Korea

<sup>2</sup> Department of Physics, University of Illinois at Urbana-Champaign, Urbana, Illinois 61801, USA

<sup>3</sup> Max-Planck-Institut für Physik komplexer Systeme, Nöthnitzer Str. 38, D-01187 Dresden, Germany

Received 24 September 2000

### Abstract

Using a three-dimensional local spin-density functional method, we investigate the electronic structure of quasi two-dimensional ellipsoidal quantum dots with elliptical deformation. Changes in the electron addition energy spectra and spin polarization are investigated as a function of the number of electrons and the elliptical deformation on the lateral direction confinement potential, and compared with those of a circular dot which shows a shell structure. Especially, we find that, due to the electron–electron interaction, the anisotropy of an elliptical dot is higher than that of a bare potential by  $\sim 1.2$  for experimentally realistic potentials.

The identification and understanding of the electronic structure of quantum dots is currently a major interest of the nanotechnology community [1,2]. In particular, single electron addition techniques together with the realization of clean and highly symmetric vertical quantum dots [3] offer the possibility to manipulate and study dots with a small well-defined adjustable number of electrons. A quasi two-dimensional (2D) shell structure, such as the enhancement of electron addition energies for certain number of electrons and spin-state variations according to Hund's first rule, is clearly observed in circular dots [3]. This experimental identification of the shell structure is also in good agreement with theoretical model calculations [4–7].

While the full rotational symmetry of a circular dot leads to the most prominent shell structure and well-defined physical pictures, there has also been other recent experimental [8] and theoretical [4,7,8] efforts to identify the role of the interplay between the circular symmetry breaking in the external potentials and the electron–electron interaction on the electronic structure of quantum dots. The finite electron addition spectra in quantum dots are closely related to the physics of single electron transistor applications, and the manipulation of the electron-spin states is also an interesting subject in magnetoelectric and optoelectric applications [2,9]. Since the presence of the asymmetry in the confining potential should be experimentally more realistic, it is important to understand the role of the symmetry breaking on the electronic structure of quantum dots due to such as an impurity [10] or the potential deformation.

In this work, we report a study of the electronic structure of three-dimensional (3D) elliptically shaped quantum dots with elliptical deformation in the lateral-direction confinement potential. Performing self-consistent total energy calculations based on the spin-dependent Kohn–Sham (KS) density functional theory (DFT) [11] in the local density approximation (LDA) [12], we observe changes in the electron addition energy spectra and spin configurations as elliptically deforming the lateral confinement potential starting from a circular dot for a fixed dot-growth direction potential. One of us (IHL) has previously performed a 3D calculation of elliptical dots, but the confinement potentials along the lateral direction employed in the work were too strong compared with experimentally realistic values [5]. Considering recent experimental developments [8] and the theoretical and technical importance of the ability to modify and understand the electronic structure of quantum dots, we report here a more detailed 3D study of the effects of the elliptical deformation on a circular quantum dot with potential parameters taken from recent experiments.

Our calculations for the quantum dots in GaAs host material (dielectric constant  $\epsilon = 12.9$ , effective mass  $m^* = 0.067m_e$ ) are based on the effective mass approximation, so that the scaled length and energy units are respectively 101.88 Å and 10.96 meV. The strong confinement along the dot-growth direction  $z$  caused by band offset in the quantum wells is assumed to be parabolic with  $\omega_z$ . The lateral confinement potential in the  $x - y$  plane is approximated by an anisotropic harmonic oscillator potential with frequencies  $\omega_x$  and  $\omega_y$ , with a constraint of  $\omega = \sqrt{\omega_x \omega_y}$  that corresponds to conserving the area of deformed quantum dots [8]. Hence, defining the ellipticity of quantum dots as the ratio of harmonic oscillator frequencies,  $\delta = \omega_x/\omega_y$ , the total external potential of our quasi 2D quantum dot can be written in the Cartesian coordinate as

$$V_{ext}(\vec{r}) = \frac{1}{2}\omega^2\left(\delta x^2 + \frac{y^2}{\delta}\right) + \frac{1}{2}\omega_z^2 z^2. \quad (1)$$

In addition to  $\omega_z = 45$  meV as in our previous investigations [5,10], experimentally realistic lateral-direction potential parameter  $\omega = 5$  meV has been chosen [8], which is significantly smaller than that of our previous investigations,  $(\omega_x, \omega_y) = (10, 20), (7, 10)$  meV. The 3D and 2D LDA exchange correlation functionals are about equally applicable in the range of  $20 \leq \omega_z/\omega \leq 30$  although 3D functional is definitely better [13] for  $\omega_z/\omega \sim 10$ . We have tested the effect of  $\omega_z$  on the electronic structure of the model by varying the  $\omega_z$  up to 65 meV. No noticeable changes in addition energy spectra are found. KS total energy calculations of  $E(N, \delta)$  for  $1 \leq N \leq 13$  have been performed with a 19-point higher-order finite-difference method and grid spacing  $h = 0.3$  a.u.\* [5,10,14], as varying  $\delta$  from 1.0 to 2.0 with an increment of 0.1. The chemical potential of an  $N$ -electron system for a fixed  $\delta$  is obtained by two different total energy calculations using the definition  $\mu(N) = E(N) - E(N-1)$  with  $\mu(1) = E(1)$ . So, the addition energy for an  $N$ -electron system,  $\Delta(N) = \mu(N+1) - \mu(N)$ , which is proportional to the gate voltage change between two successive conductance peaks in Coulomb oscillation measurements, is obtained by three different total energy calculations

$$\begin{aligned} \Delta(N) &= \mu(N+1) - \mu(N) \\ &= E(N+1) + E(N-1) - 2E(N). \end{aligned} \quad (2)$$

We first consider variations of chemical potentials and single electron addition energy spectra with elliptical deformation of the dot. Variations of  $\mu(N)$  versus  $\delta$  are shown in figure 1, which reminds one of the chemical potential dependence on the magnetic field [2]. The first three lines vary monotonically, while other higher lines fluctuate up and down with the increase of deformation parameter. We further observe that they shift in pairs, which is also analogous to the chemical potential variation with the magnetic field. We also obtain  $\Delta(N)$  for a fixed  $\delta$  (using equation 2), which corresponds to the spacing between the  $\mu(N)$

and  $\mu(N+1)$  lines in figure 1. These are shown for  $\delta = 1.3, 1.5, 1.7,$  and  $2.0$  in figure 2 together with that of the circular dot ( $\delta = 1$ ). In a circular dot,  $\Delta(N)$  spectra show large peaks for certain numbers of electrons, especially for  $N = 2, 6,$  and  $12$ , which represent shell structures [3,5]. These peaks are still observed, but are much more suppressed for  $\delta = 1.1$ . For  $\delta = 1.2$ , they are more suppressed and the  $N = 12$  peak disappears first. For further deformations, e.g.  $\delta = 1.3$ , most peaks of the circular dot are washed out except for  $N = 2$  as shown in figure 2. However, interestingly, we again observe pronounced peaks especially at  $N = 4, 8,$  and  $12$  for  $\delta = 1.7$ . These newly formed peaks subsequently disappear with further deformations.

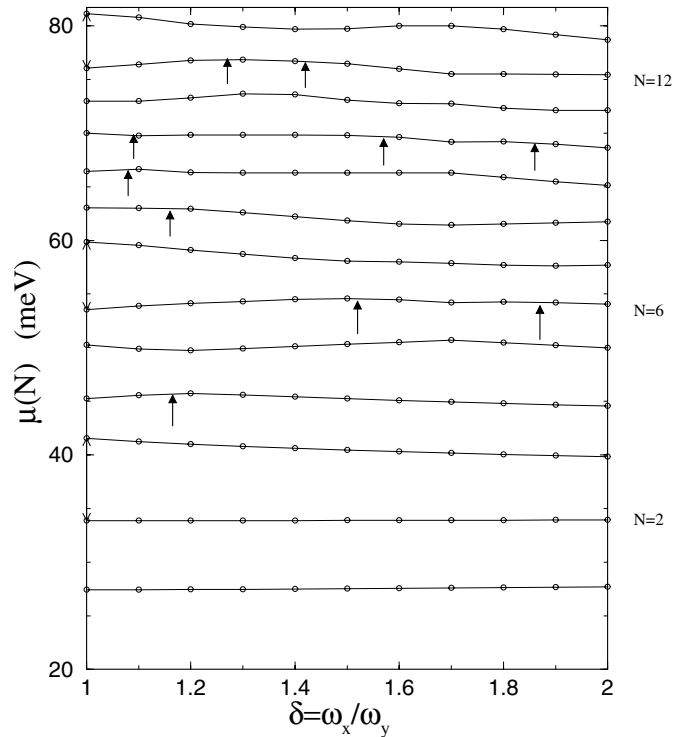


**Figure 1.** Calculated chemical potentials  $\mu(N) = E(N) - E(N - 1)$  versus the deformation parameter  $\delta = \omega_x/\omega_y$ . The lowest line  $\mu(1)$  is the total energy of the single-electron system  $E(1)$ . Upward arrows denote the critical deformation parameters  $\delta_c$  where spin configurations change.

Another variable of interest is the total spin of the ground states. Spin configurations in the circular dot follow the Hund's rule in open-shell regions [3,5], and change as  $(\frac{1}{2} \rightarrow 0) \rightarrow (\frac{1}{2} \rightarrow 1 \rightarrow \frac{1}{2} \rightarrow 0) \rightarrow (\frac{1}{2} \rightarrow 1 \rightarrow \frac{3}{2} \rightarrow 1 \rightarrow \frac{1}{2} \rightarrow 0) \rightarrow \frac{1}{2}$ , where parentheses indicate shells as will be discussed later. As the dot is deformed, we find variations in the ground-state spin state by 1 for certain  $N$ ,  $S(N)$ , at the critical deformation parameter,  $\delta_c(N)$ , as shown in figure 1. Critical deformation parameter values are indicated by upward arrows. Note that we do not have spin-state variations for odd-number of electrons except  $S(9) = \frac{3}{2} \rightarrow \frac{1}{2}$  at very small deformation  $\delta_c(9) = 1.08$ . On the other hand we observe variations in spin configuration for all even- $N$  electrons except  $S(2) = 0$ :  $S(4) = 1 \rightarrow 0$  at  $\delta_c(4) = 1.17$ ,  $S(6) = 0 \rightarrow 1 \rightarrow 0$  at  $\delta_c(6) = 1.52$  and  $1.87$ ,  $S(8) = 1 \rightarrow 0$  at  $\delta_c(8) = 1.16$ ,  $S(10) = 1 \rightarrow 0 \rightarrow 1 \rightarrow 0$  at  $\delta_c(10) = 1.09, 1.57,$  and  $1.86$ , and, finally,  $S(12) = 0 \rightarrow 1 \rightarrow 0$  at  $\delta_c(12) = 1.27$  and  $1.42$ . Hence, in figure 1 we find two main regions where spin-state changes in an interesting manner: one is at  $\delta \sim 1.0$  with spin-state

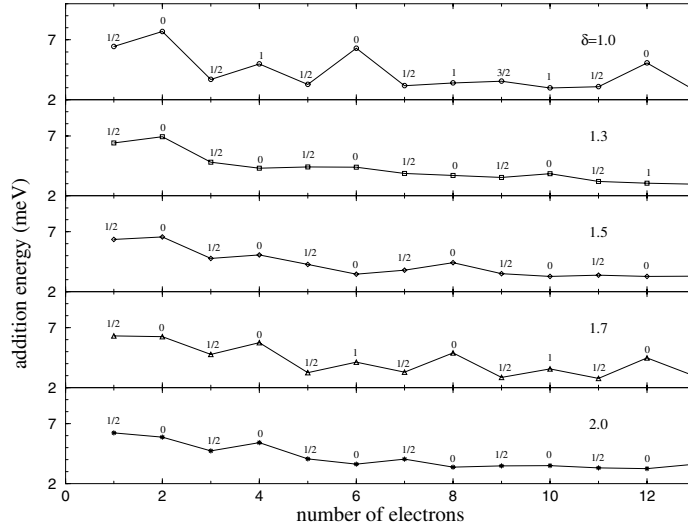


**Figure 2.** Addition energies  $\Delta(N) = \mu(N+1) - \mu(N)$  versus the number of electrons  $N$  for  $\delta = 1.0, 1.3, 1.5, 1.7,$  and  $2.0$ .

variation as mentioned above, and the other is  $\delta \sim 1.6 - 1.8$  with a spin configuration change as  $(\frac{1}{2} \rightarrow 0) \rightarrow (\frac{1}{2} \rightarrow 0) \rightarrow (\frac{1}{2} \rightarrow 1 \rightarrow \frac{1}{2} \rightarrow 0) \rightarrow (\frac{1}{2} \rightarrow 1 \rightarrow \frac{1}{2} \rightarrow 0) \rightarrow \frac{1}{2}$ . Note that these two parameter ranges are where large  $\Delta(N)$  peaks are found in figure 2. For most other ranges of  $\delta$ , spin polarizations oscillate between  $S = \frac{1}{2}$  and 0 as electrons are added, except for  $\delta \sim 1.1$  with  $\frac{1}{2} \rightarrow 0 \rightarrow \frac{1}{2} \rightarrow 1 \rightarrow \frac{1}{2} \rightarrow 0 \rightarrow \frac{1}{2} \rightarrow 1 \rightarrow \frac{1}{2} \rightarrow 0 \rightarrow \frac{1}{2} \rightarrow 0 \rightarrow \frac{1}{2}$ , which is a variation of  $\delta = 1$  spin-state variation, and for  $\delta \sim 1.3$  with  $\frac{1}{2} \rightarrow 0 \rightarrow \frac{1}{2} \rightarrow 0 \rightarrow \frac{1}{2} \rightarrow 0 \rightarrow \frac{1}{2} \rightarrow 0 \rightarrow \frac{1}{2} \rightarrow 1 \rightarrow \frac{1}{2}$ .

Now, we argue that these changes of electron addition energy spectra and spin-state variations with elliptical potential deformation can be understood by observing the development of single-particle energy states. First, we consider the noninteracting system whose (doubly degenerate) eigenvalues with the deformation are given in figure 3. In the circular dot ( $\delta = 1$ ), eigenvalues have doubly and triply degenerate second and third set of states (A and B), which are equally separated by  $\omega = 5$  meV and will be completely filled for  $N = 6$  and 12. With the deformation in the lateral confinement potential, degeneracies of single-particle states associated with the circular symmetry of the potential are lifted, and the spacings between single-particle states in different degeneracy groups of the circular dot become smaller. However, note that the eigenvalues develop degeneracies at two other deformation parameter values,  $\delta = 1.5$  and 2.0. At  $\delta = 1.5$ , they are doubly degenerate at the sixth state (C), and will be completely filled at  $N = 14$ . At  $\delta = 2.0$ , degeneracies of the noninteracting eigenstates occur at the third and fifth levels (D and E), each of which should be completely filled for  $N = 8$  and 12 electrons.

Circular dots, 2D shell structures described above, such as spin compensations and large  $\Delta(N)$  at  $N = 2, 6,$  and  $12$ , analogous to He, Ne, and Ar in the atomic physics, and the Hund's rule spin-state variation, are experimentally observed [3], and are known to be well accounted for by the noninteracting eigenvalue spectrum, a constant interaction, and corrections due to the exchange. Assuming that the noninteracting picture of eigenvalue spectra in figure 3 is also transferred in other ranges of deformation parameter values, we expect the breaking of the shell structure in the circular dot with deformation, or the decrease of the peaks in the electron

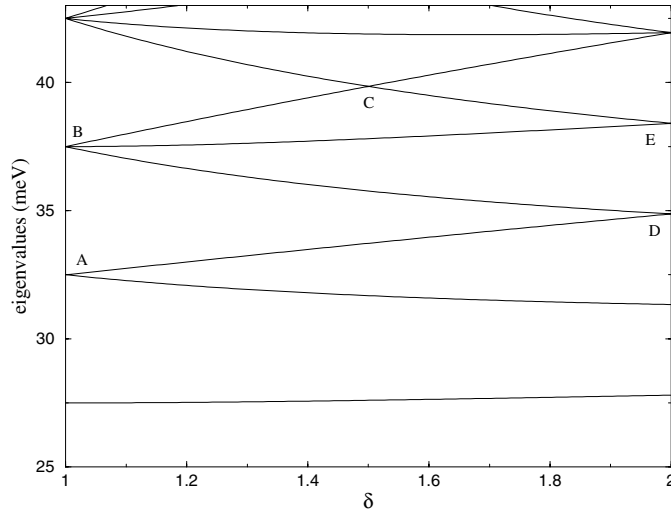


**Figure 3.** Noninteracting single-particle eigenvalues as a function of  $\delta$ . Each state is doubly spin-degenerate. Lines indicate the states relevant to our study of  $N$  up to 13. A, B, C, D, and E are degenerate points. See the text.

addition energy spectra and the break-down of Hund's rule spin-state variations. With further deformation, however, we can expect the Hund's rule spin-state variation at  $\delta = 1.5$ , and pronounced shell structures, or enhanced addition energies at  $N = 4, 8$ , and  $12$ , and Hund's rule spin-state variation,  $(\frac{1}{2} \rightarrow 0) \rightarrow (\frac{1}{2} \rightarrow 0) \rightarrow (\frac{1}{2} \rightarrow 1 \rightarrow \frac{1}{2} \rightarrow 0) \rightarrow (\frac{1}{2} \rightarrow 1 \rightarrow \frac{1}{2} \rightarrow 0) \rightarrow \frac{1}{2}$ , at  $\delta = 2.0$ . Note that there are two main physically competing effects in these descriptions: one is the energy lowering by the exchange coupling, the maximum of which is obtained in degenerate states present when the symmetry of the external potential is dominant. The other is that by the splitting of eigenvalues with introduction of asymmetry in the external potential, which lowers the total energy by making an electron, which was formerly in a degenerate state of a symmetry case, to be able to occupy the lower-energy level state.

Comparing these descriptions based on the noninteracting eigenvalue spectra with our calculation results, we observe that the general picture holds well, but with  $\delta$  shifted to smaller values: spin-polarized state at  $N = 12$  occurs at  $\delta \sim 1.3$  rather than at  $1.5$ . Also, another shell structure, such as pronounced addition energies at  $N = 4, 8$ , and  $12$  and the spin-configuration variation according to Hund's rule, are observed at  $\delta \sim 1.7$  rather than at  $2.0$ . So, we can conclude that the effective potential, or the self-consistent potential, of elliptically shaped dots is more anisotropic than that of the bare potential due to the electron–electron interaction by  $\delta_{eff}/\delta_{bare} \sim 1.15 - 1.25$ , or the electron–electron interaction supports more elongated electron configurations along the weak confinement potential axis in deformed quantum dots.

Now, to make the above findings more quantitative, we consider the LDA KS eigenvalues for the 12 electron system for different values of deformation parameter  $\delta$  shown in figure 4. Before proceeding, we approximately identify the highest occupied (HO) and lowest unoccupied (LU) eigenvalues of  $N$ -electron system as the chemical potentials of  $N$  and  $N + 1$  electron systems [11]:

$$\mu(N) \approx \epsilon_{HO}^{LDA}(N) \quad \mu(N + 1) \approx \epsilon_{LU}^{LDA}(N). \quad (3)$$

While we have to remind the reader that the LDA KS eigenvalues do not have any strict physical meaning, [11] we expect these relations will give a good qualitative picture of interacting systems. Then, the  $(N + 1)$ -th electron-addition energy for an  $N$ -electron system,  $\Delta(N)$ , is approximately equal to  $\epsilon_g^{LDA}(N) \equiv \epsilon_{LU}^{LDA}(N) - \epsilon_{HO}^{LDA}(N)$ . Now, in figure 1 for  $N = 12$ , we find that the originally triply degenerate third level ( $N = 7 - 12$ ) in the noninteracting description for  $\delta = 1.0$  is transformed into a two-fold degenerate third state ( $N = 7 - 10$ ) and a single fourth state ( $N = 11 - 12$ ) after the inclusion of electron–electron interaction. Big  $\epsilon_g^{LDA}(12)$  at  $\delta = 1.0$  indicates a large addition energy and subshell closure observed in figure 2. Note a similar behaviour of eigenvalue spectra, a signature of the shell-structure, at  $\delta = 1.7$  instead of  $\delta = 2.0$ , which confirms that the effective ellipticity of a self-consistent potential is larger than that of a bare potential. In addition, the splitting between up and down electron eigenvalue spectra and the collapse of  $\epsilon_g^{LDA}(12)$  at  $\delta = 1.3$ , which represents a spin polarization  $S(12) = 1$ , indicates that the effective ellipticity of the interacting system at  $\delta = 1.3$  corresponds to that of the noninteracting system at  $\delta = 1.5$  in figure 3.

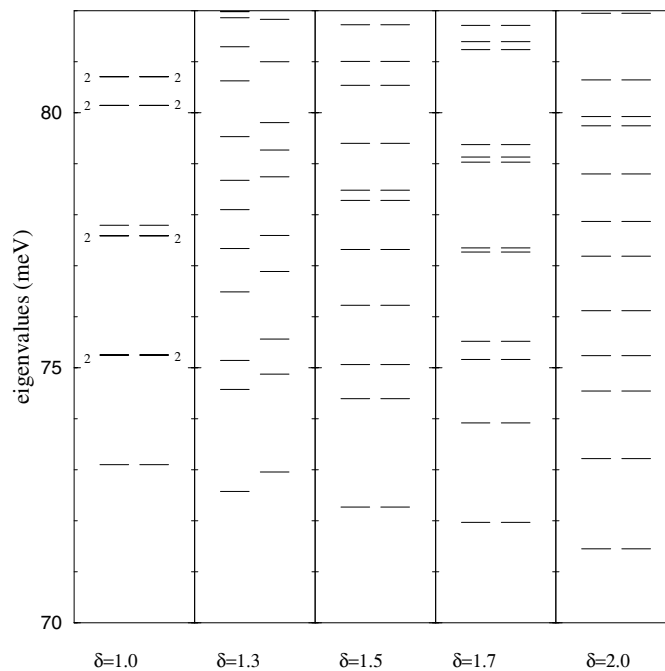


**Figure 4.** The development of KS LDA eigenvalues for the 12-electron system with  $\delta$ . Left and right horizontal lines represent the eigenvalue spectra of spin-up and -down states. Total spin-state for  $\delta = 1.3$  is  $S(12) = 1$ . The degeneracy factor 2 in the panel for  $\delta = 1.0$  represent doubly degenerate states.

Finally, we comment on the connection between our work and a recent experimental study in [8]. Austing *et al* suggested that the anisotropy of their elliptically shaped dots in practice can be much higher than that given by simply considering the geometry of the device mesa in which the dot is located by observing the magnetic field dependence [8]. Hence, our calculations can be considered as a direct confirmation of their proposition. However, we also note that the ellipticity of their dots are not well-defined, and determining  $\delta$  is quite hard in the experiments. Actually, the geometry of their dots are rectangular rather than elliptical,

hence direct comparisons, for example between their addition energy data and our calculation results, is not possible. Based on our study, we may suggest that when manufacturing a dot in the signature of the shell structure of  $\delta = 2.0$ , it is found that we can confirm the degree of elliptical symmetry of their dots and give a definite relationship between  $\delta$  and geometrical values.

In summary, we have studied the electronic structures of ellipsoidally deformed quantum dots with 3D local spin-density functional calculations. They indicate that the elliptical-deformation on a circular dot in general breaks the shell structure and significantly affects its electronic structure. Calculation results are explained by examining the development of the non-interacting and the corresponding KS single-particle energy spectra with the deformation on external potentials. Especially, we find that the anisotropy of an elliptical dot is higher than that of a bare potential by  $\delta_{eff}/\delta_{bare} \sim 1.2$  due to the electron–electron interaction in the experimentally realistic external potential parameters, which is in agreement with the recent suggestion based on the magnetic field dependence experiments [8].

### Acknowledgments

IHL acknowledges support for this work by the supercomputer centre KORDIC.

### References

- [1] Ashoori R C 1996 *Nature* **379** 413
- [2] Kouwenhoven L P, Marcus C M, McEuen P L, Tarucha S, Westervelt R M and Wingreen N S 1997 *Mesoscopic Electron Transport* ed. L L Sohn, L P Kouwenhoven and G Schön (Dordrecht: Kluwer Academic)
- [3] Tarucha S, Austing D G, Honda T, van der Hage R J and Kouwenhoven L P 1996 *Phys. Rev. Lett.* **77** 3613
- [4] Ezaki T, Mori N and Hamaguchi C 1997 *Phys. Rev B* **56** 6428
- [5] Lee I-H, Rao V, Martin R M and Leburton J-P 1998 *Phys. Rev B* **57** 9035
- [6] Steffens O, Rössler U and Suhrke M 1998 *Europhys. Lett.* **42** 529
- [7] Hirose K and Wingreen N S 1999 *Phys. Rev B* **59** 4604
- [8] Austing D G, Sasaki S, Tarucha S, Reimann S M, Koskinen M and Manninen M 1999 *Phys. Rev B* **60** 11 514
- [9] Di Vincenzo D 1995 *Science* **270** 255
- [10] Lee I-H, Ahn K-H, Kim Y-H, Martin R M and Leburton J-P 1999 *Phys. Rev B* **60** 13 720
- [11] Parr R G and Wang W 1989 *Density Functional Theory of Atoms and Molecules* (Oxford: Oxford University Press)
- [12] Dreizler R M and Gross E K U, *Density Functional Theory* 1990 (Berlin: Springer)
- [13] Ceperley D M and Alder B J 1980 *Phys. Rev. Lett.* **45** 566
- [14] Perdew J and Zunger A 1981 *Phys. Rev B* **23** 5048
- [15] Kim Y-H, Lee I H, Nagaraja S, Leburton J-P, Hood R Q and Martin R M 2000 *Phys. Rev B* **61** 5202
- [16] Lee I-H, Kim Y-H and Martin R M 2000 *Phys. Rev B* **61** 4397